Science of the Total Environment 760 (2021) 144149

Contents lists available at ScienceDirect

Science of the Total Environment

journal homepage: www.elsevier.com/locate/scitotenv

Impacts of bark beetle-induced tree mortality on pyrogenic carbon production and heat output in wildfires for fire modeling and global carbon accounting

Alexandra Howell [a], Mario Bretfeld [b], Erica Belmont [a,*]

[a] Department of Mechanical Engineering, The University of Wyoming, 1000 E. University Ave., Laramie, WY, USA
[b] Department of Ecology, Evolution, and Organismal Biology, Kennesaw State University, 370 Paulding Ave., Kennesaw, GA, USA

HIGHLIGHTS

- Pyrogenic carbon (PyC) is a potentially significant atmospheric carbon sink.
- Wildfire impacts on healthy and beetle-killed lodgepole pine boles were compared.
- Bark beetle disturbances influence pyrolysis kinetics and increase charring extents.
- Fuel composition changes due to beetle disturbance enhance PyC production from fire.
- Impacts at bole-level were scaled to assess ecosystem-level implications.

GRAPHICAL ABSTRACT

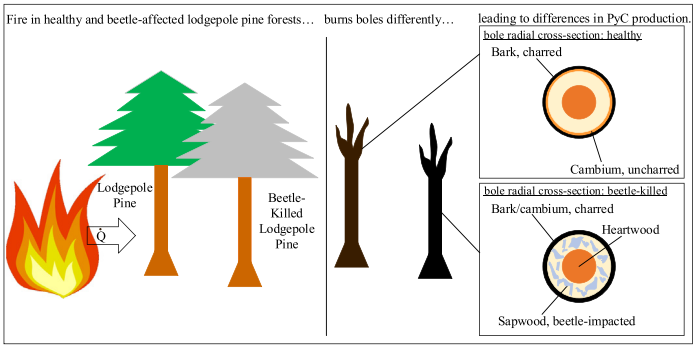

ARTICLE INFO

Article history:
Received 16 October 2020
Received in revised form 24 November 2020
Accepted 25 November 2020
Available online 9 December 2020

Editor: Manuel Esteban Lucas-Borja

Keywords:
Wildland fire
PyC
Carbon sink
Dendroctonus ponderosae
Pinus contorta
Pyrolysis kinetics

ABSTRACT

Forests store significant quantities of carbon, and accurate quantification of the fate of this carbon after fire is necessary for global carbon accounting. Pyrogenic carbon (PyC) encompasses various carbonaceous products of incomplete combustion formed during fires and has potential to act as a carbon sink for up to millennia, but current estimates of PyC production in wildfires vary widely. Northern hardwood forests have changed dramatically in recent decades due to insect epidemics, such as the bark beetle epidemic in the Rocky Mountain Region which has caused widespread mortality. This study assessed impacts of bark beetle-induced mortality on fuel pyrolysis kinetics, carbon partitioning of combustion products, and net heat output to aid in forest fire modeling and carbon accounting by comparing healthy and beetle-killed lodgepole pine tree boles burned in a 2018 forest fire in southeast Wyoming, USA with unburned boles. Results showed charring predominantly restricted to the bark and cambium. Significant differences between burned and unburned healthy and beetle-impacted bark/cambium compositions were identified, and PyC production and energy output were quantified. Charring extent and PyC content were found to be greater in beetle-impacted boles due to a reduction in bark/cambium resistance to heating and charring, with 80 times more PyC produced in a beetle-killed bark/cambium than in a healthy bark/cambium. Upon scale-up, total PyC production in the fire-affected area was estimated to be 0.71 GgPyC (82.5 kgPyC/ha). This was found to be significantly enhanced compared to an estimated PyC production of 0.036 GgPyC (4.12 kgPyC/ha) in a hypothetical healthy lodgepole pine ecosystem of equal area. The results of this investigation concluded that the 58% beetle-induced mortality in the Badger Creek Fire area resulted in 3 times more carbon released to the global atmosphere, 20 times more PyC retained onsite and 32% greater heat output during wildfire.

* Corresponding author.
E-mail address: ebelmont@uwyo.edu (E. Belmont).

https://doi.org/10.1016/j.scitotenv.2020.144149
0048-9697/

1. Introduction

Wildfires emit approximately 2.2 Pg of carbon into Earth's atmosphere each year (Jones et al., 2019; Hobley et al., 2017), and wildfire frequency and severity are projected to increase in many regions as climates change (Hobley et al., 2017; Santín et al., 2015). Accurate quantification of the fate of forest carbon reserves during wildfires, whether emitted to the atmosphere or left in situ, is needed for global carbon balance models (Hobley et al., 2017; Meigs et al., 2015). More accurate estimates of carbon partitioning for a variety of vegetation and fire conditions could help reconcile the missing sink of ~1.5 PgC per year in current atmospheric models, which do not account for the pyrogenic carbon (PyC) produced during wildfires (Hobley et al., 2017; Donato et al., 2009). PyC consists of a wide range of carbonaceous species formed during incomplete combustion and retained in soot and char after fires. Although the PyC continuum encompasses chemical compounds that can be highly labile or highly stable, ranging from charred biomass and charcoal to soot and graphite, it is generally agreed upon as being carbon-rich and recalcitrant to environmental degradation with the potential to sequester carbon up to a time scale of millennia (Meigs et al., 2015; Santín et al., 2016; Santín et al., 2017; Knicker et al., 2008).

Important aspects of wildfires, including carbon fate and fire dynamics, are directly impacted by feedstock characteristics. Heterogeneity of wildland fuels and burning conditions make modeling wildland fire a complex undertaking because a large number of interacting chemical and physical processes must be considered both spatially and temporally (Donato et al., 2009; Chatterjee et al., 2012). Biomass combustion occurs via two major steps: pyrolysis, producing volatile species or pyrolyzates that undergo homogenous gas-phase combustion, and heterogeneous oxidation of the remaining solid char by ambient gases. Fire intensity and spread are directly related to the rate and amount of heat release from pyrolyzate combustion, which promote further fuel pyrolysis and sustain the fire. The heat release from pyrolyzate combustion therefore also promotes further fuelwood charring, which is the principal mechanism for PyC production, while heterogeneous oxidation is a mechanism for its consumption (Pérez-Ramirez et al., 2012; Albini, 1980; Albini, 1976; Law, 2006). The composition and combustion kinetics of the pyrolyzates are influenced by a broad range of factors including vegetation composition, weather conditions and available oxygen within the burning environment. Consequently, the rates, extents and final chemical forms of PyC production are influenced by the heating conditions undergone by the unburned fuels, leading to devolatilization and ignition, as well as heterogeneous oxidation and smoldering after the fire front has passed (Santín et al., 2015; Pérez-Ramirez et al., 2012; Albini, 1976; López-Martín et al., 2018).

With increasing pyrolysis temperatures and durations, greater amounts of increasingly aromatic PyC are formed by condensation and cross-linking of soot and soot precursors on residue surfaces (Schimmelpfennig and Glaser, 2011; Preston and Schmidt, 2006). The final carbon structures and amounts of aromatics in the PyC then determine its stability and recalcitrance to environmental degradation. After the fire, PyC can be transported and relocated, and undergo size reduction via aerial and fluvial processes, but mechanisms for its deterioration post-wildfire, such as rapid consumption in subsequent wildfire or slow microbial degradation (Preston and Schmidt, 2006; Goldberg, 1985), are limited. Thus, PyC stocks in soils can act as durable carbon sinks after fire (Hobley et al., 2017; Santín et al., 2016; Gale and Thomas, 2019).

Field data to enhance and test existing wildland fire models, specifically models that predict spread rates and products of fire, are difficult to obtain and, as a result, models must often utilize data obtained from laboratory fire experiments (Santín et al., 2017; Alexander and Cruz, 2013). Biochar produced via pyrolysis in laboratory studies may not be representative of wildland fire conditions, however, which are often characterized by high intensity, short duration, and partial combustion of biomass (Santín et al., 2017; Albini, 1976; Schimmelpfennig and Glaser, 2011). Additionally, although fire spread is governed by the complex composition and combustion kinetics of fuel pyrolyzates, reduced global reaction mechanisms are often employed in models (Pérez-Ramirez et al., 2012; Berner et al., 2012; Keeley, 2009; Tihay et al., 2009). Computational costs limit these models to the consideration of only a few representative gas species, such as CO and H_2, and one- or two-step global reaction schemes. This approach necessarily results in a loss of accuracy because reactant species composition is a key determinant of flame kinetics. Heats of combustion of the volatile gases are typically considered to range from 12,000 to 16,000 kJ/kg (Pérez-Ramirez et al., 2012); however, more accurate quantification of key characteristics of pyrolyzates, such as the heat output from combustion of these gas-phase mixtures, is needed for improved modeling (Pérez-Ramirez et al., 2012; Berner et al., 2012; Keeley, 2009).

Many forests worldwide are experiencing heightened disturbances from insects due to hotter and drier climates (Jenkins et al., 2014). Among these insect disturbances, the recent mountain bark beetle (*Dendroctonus ponderosae*) epidemic in the Rocky Mountain region has affected 558 billion m^3 of standing timber and induced a 32% tree mortality (Berner et al., 2012; Harvey et al., 2014). There has been extensive investigation into the impacts of these disturbances on fire frequency, fire severity and carbon fluxes, but the interactions between insect- and fire-disturbances and forest fuel composition are complex and still not fully understood (Berner et al., 2012; Jenkins et al., 2014; Harvey et al., 2014; Page and Jenkins, 2007; Edburg et al., 2012; Jenkins et al., 2008; Klutsch et al., 2009). Additionally, there have been few studies investigating the production of PyC from wildfires (Santín et al., 2015; Santín et al., 2016) and no studies investigating the interactions of wildfire, PyC production and beetle-induced mortality. To date, interactions between bark beetle disturbance and fire remain controversial as increased, decreased and no relationships have been found in various studies, depending on the outbreak stage, ecosystem type and burning conditions (Meigs et al., 2015; Jenkins et al., 2014; Jenkins et al., 2008; Klutsch et al., 2009; Liang et al., 2016; Bond et al., 2009; Simard et al., 2011). Among the difficulties in assessing bark beetle impacts on fire is the challenge of procuring appropriate controls (Harvey et al., 2014). The wildfire that impacted 21,310 acres in the Badger Creek watershed of the Medicine Bow-Routt National Forest in southeastern WY, USA, in June and July of 2018 (*Badger Creek Fire*, 2018) offered an opportunity to study bark beetle impacts with controls provided by the nature of the forest itself, as the forest in this region is dominated by even-aged lodgepole pine (*Pinus contorta*) that has been heavily affected by bark beetles, with most tree mortality occurring over a three-year window between 2008 and 2011 (Kipfmueller and Baker, 2000; Kayes and Tinker, 2012). This region was also heavily instrumented before the fire by University of Wyoming researchers to investigate effects of the bark beetle on lodgepole pine forest ecosystems, providing detailed pre-fire beetle infestation data (Kayes and Tinker, 2012; Reed et al., 2014).

This study investigated differences in pyrolysis kinetics, carbon partitioning, PyC formation and net heat output between beetle-killed and healthy lodgepole pine (BK and HP, respectively) during the Badger Creek Fire in order to provide better estimates for carbon accounting and improved inputs for wildfire spread models. PyC contained in standing timber aboveground has demonstrated greater mean residence times in situ than that produced from downed trees and finer fuel particles (Rumpel et al., 2015; Ohlson et al., 2009), but there is still significant uncertainty in quantification of formation magnitudes. Thus, tree boles were investigated in this study to better assess retained PyC. Charring severity, carbon content and PyC production were compared between burned and unburned BK and HP boles to quantify amounts of carbon released and retained. Detailed analyses of elemental, fixed and volatile carbon, and PyC, as well as quantification of energy released during the fire were performed. Isoconversional kinetic rate parameters were derived to elucidate differences in pyrolysis kinetics induced by bark beetle infestation. The heat output and carbon partitioning analyses were employed to assess large-scale fire impacts of lodgepole pine and beetle-affected forest ecosystems.

2. Materials and methods

2.1. Materials

Burned and unburned beetle-killed (BK) and healthy (HP) lodgepole pine boles were obtained from the Medicine Bow-Routt National Forest near Chimney Park Scout Camp, which is near the Badger Creek Fire boundary. Burned and unburned boles were collected in May/June of 2019, ten months after the fire. Burned boles were attained within the fire boundary and unburned samples were collected from immediately outside the fire-affected area to ensure all samples were obtained from an even-aged, relatively homogenous lodgepole pine stand. Beetle-killed trees were in the gray stage of the epidemic outbreak at the time of the fire. A total of 12 boles (three each of burned and unburned BK and HP) of approximately 16.5 cm in diameter and 1.0 m in length were collected. Bole cross sections were cut to capture fire impacts and charring at an average bole height of 1.0 m. Radial regions of each bole were identified as bark/cambium, sapwood and heartwood (Fig. 1a). The bark/cambium region consisted of both the bark and the cambium layer immediately adjacent to the bark (Fig. 1b and c).

The bark/cambium regions were visually distinct between beetle-affected and healthy samples due to relative loss of moisture and lack of malleability in beetle-affected boles, and burned or unburned samples due to charring in burned boles. The bark/cambium layer in burned healthy pine was characterized by charred bark and uncharred cambium (Fig. 1b), while the burned beetle-killed pine was characterized by charring that extended through the cambium (Fig. 1c). The sapwood was visually characterized as being either affected or unaffected by residues of the blue-stain fungi (*Ophiostoma clavigerum* and *Ophiostoma montium*) related symbiotically to, and providing evidence of, the presence or absence of the bark beetle (Solheim and Krokene, 1998). The heartwood layer was visually similar between all boles. In order to determine the changes in properties due to charring extent during the Badger Creek Fire, all bole layers underwent proximate analysis. Particles of approximately 1–2 mm in diameter were extracted from each of the three radial bole layers (bark/cambium, sapwood and heartwood) for each of the four bole categories (burned and unburned HP and BK). The bark/cambium was sampled together as a single layer and samples beyond the bark/cambium were obtained at 1 cm radial increments.

2.2. Proximate analysis

A TA Instruments Q500 thermogravimetric analyzer (TGA) was utilized to conduct proximate analysis following the KAR procedure (García et al., 2013). HP and BK bark/cambium, sapwood and heartwood samples were dried at 100 °C in 99.99% purity nitrogen (N_2) for 10 min to measure the moisture content (MC) by mass loss, then ramped to 950 °C at 40 °C/min and held isothermal for 7 min. The mass loss that occurred during this high temperature step reflects the volatile content (VC) of the samples. Lastly, the TGA furnace was cooled to 750 °C and an oxygen (O_2, 99.9% purity) and N_2 mixture was introduced to the furnace at a 20/80 *v*/v% to simulate air and combust the samples. The remaining mass after combustion is the ash content (AC), and the fixed carbon (FC) content is obtained from the balance of the initial sample mass (García et al., 2013). FC is a measure of the condensed, non-volatile carbon that remains in a sample after it has lost its labile compounds due to heating. Although FC is not a direct measure of PyC content, FC and VC are indicators of the extent of charring that a feedstock underwent in wildfire conditions. Relative values of VC and FC between unburned and burned boles can therefore give insights into expected trends of PyC contents post-fire (García et al., 2013). FC and VC were normalized and are reported on a dry, ash-free (DAF) basis. A minimum of three replicates were performed for each bole layer (bark/cambium, sapwood and heartwood) of each sample type (burned and unburned HP and BK). All uncertainty in this study was assessed using the Student's *t*-test with a 95% confidence interval. Based upon the quantitative results of this proximate characterization, all ensuing characterization methods were restricted to the bark/cambium of each bole sample.

2.3. Isoconversional kinetic analysis

Numerous TGA-based methods for deriving Arrhenius kinetic parameters of pyrolysis reactions have been developed and used to good effect (Tihay and Gillard, 2011; Arenas et al., 2019; Leroy et al., 2006). Isoconversional techniques like the Ozawa-Flynn-Wall (OFW) technique, however, are particularly adept at modeling reaction rate parameters as functions of reaction temperature and conversion extent and have been recommended for the modeling of pyrolysis kinetics under wildfire conditions (Tihay and Gillard, 2011; Arenas et al., 2019). Heating rates observed during wildfires are highly variable, ranging from slow smoldering to rapid crown fire spread under high wind velocities (Pyne et al., 1996). Isoconversional models capture the changes in the reaction mechanism experienced at different heating rates by reporting kinetic parameters as a function of the degree of conversion and the temperature realized by the fuel at that conversion (Tihay and Gillard, 2011; Arenas et al., 2019).

The OFW isoconversional technique was used in this study to assess the kinetic parameters for pyrolysis of unburned BK and HP. TGA was used to pyrolyze the BK and HP samples by first subjecting the samples to a 10 min drying step at 100 °C followed by a temperature ramping step to 650 °C in 99.99% purity N_2. Five different heating rates were investigated for the ramping step: 5, 10, 20, 40, and 60 °C/min. Using a

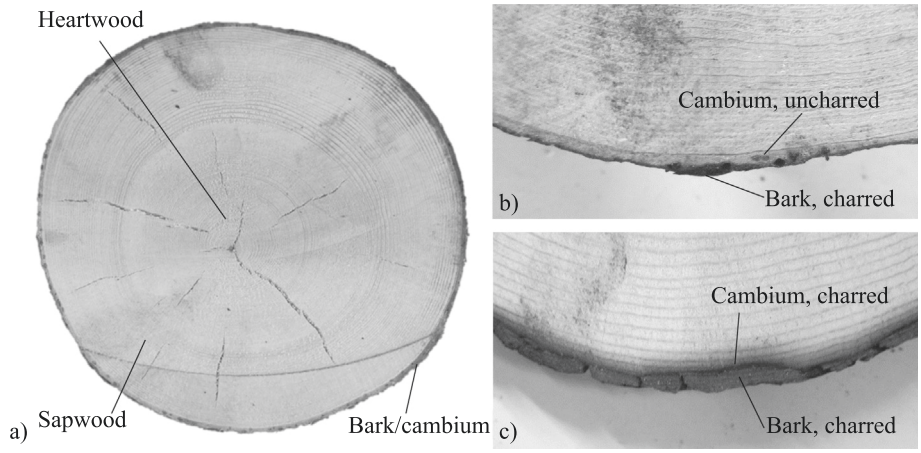

Fig. 1. Planar views of a) unburned healthy lodgepole pine bole to show radial delineation of bark/cambium, sapwood and heartwood, and bark and cambium of b) burned healthy pine and c) burned beetle-killed pine.

field heat flux sensor, Frankman et al. (2012) reported maximum radiative and convective heat fluxes of 300 and 42 kW/m^2, respectively, during crown fire in mature lodgepole pine (Rat Creek Fire 16, August 2007). These maximum fluxes correspond to radial heating rates to the boles on the order of 100 °C/min. Thus, this study utilized heating rates higher than the typical upper limit of around 30 °C/min applied in kinetic analyses (Tihay and Gillard, 2011; Arenas et al., 2019) in order to more closely approximate wildfire conditions and assess the performance of the OFW technique at higher heating rates. A summary of the OFW technique follows.

The general expression for the kinetics of heterogeneous reactions is

$$\frac{d\alpha}{dt} = \beta\frac{d\alpha}{dT} = f(\alpha)Aexp\left(-\frac{E_a}{RT}\right) \quad (1)$$

where α is the degree of conversion, t is time, β is the heating rate, $f(\alpha)$ is the differential conversion function that may be approximated by an analytical reaction model, E_a is the activation energy, A is the pre-exponential factor, and R is the universal gas constant. The degree of conversion is determined by

$$\alpha = \frac{m_0 - m}{m_0 - m_\infty} \quad (2)$$

where m_0 is the initial dry mass, m is the instantaneous mass and m_∞ is the ending mass at 650 °C. The OFW is a model-free approach such that, instead of assuming or attempting to derive a form of $f(\alpha)$, Eq. (1) is integrated to separate the terms depending on α and T as shown in Eq. (3).

$$G(\alpha) = \int_0^\alpha \frac{d\alpha}{f(\alpha)} = \frac{A}{\beta}\int_{T_0}^{T} \exp\left(\frac{-E_a(\alpha)}{RT}\right)dT = \frac{AE_a(\alpha)}{R\beta}p(x) \quad (3)$$

In this manner, the isoconversional method models the reaction rate at a specific degree of conversion only as a function of temperature. In this integrated form, if $x = E_a(\alpha)/RT$,

$$p(x) = \frac{\exp(-x)}{x} - \int_{-x}^{\infty}\frac{\exp(x)}{x}dx \quad (4)$$

and, thus, $G(\alpha)$ has no analytical solution and must be resolved using an approximation. For the OFW method, the Doyle approximation is applied:

$$\ln(p(x)) = -5.3308 - 1.0516x \quad (5)$$

The integrated form of Eq. (1) using the Doyle approximation yields the OFW isoconversional mathematical form

$$\ln\beta = \ln\left(\frac{AE_a(\alpha)}{R}\right) - \ln(G(\alpha)) + 5.331 - \frac{1.052E_a(\alpha)}{RT}. \quad (6)$$

The attainment of E_a, in kJ/mol, and $\ln(A)$ is achieved by plotting $\ln\beta$ against $1000/T$ isoconversional lines, obtained by TGA. The slope, m_{iso}, of the lines yields the activation energy by

$$E_a = \frac{m_{iso}R}{-1.052}\left[\frac{kJ}{mol}\right] \quad (7)$$

and the y-intercept gives $\ln(A)$.

2.4. Ignition temperature and char oxidation rate

To better elucidate the relationship between the kinetic parameters and volatile contents, ignition onset temperatures and char oxidation rates were investigated. Ignition temperatures and oxidation rates were obtained by heating dried unburned BK and HP bark/cambium samples to 500 °C at 10 °C/min using TGA in a simulated air environment (20/80 v/v% O_2/N_2) to emulate atmospheric conditions during the wildfire event. Six replicates were performed for both BK and HP. Stage 1 and 2 ignition temperatures were defined at the first and second maximums of the derivative mass loss curves, respectively, where Stage 1 represents volatile ignition and Stage 2 represents char oxidation. Char oxidation rate was determined as the change in mass % over the change in time from the start of heterogeneous char oxidation (Stage 2 ignition) to the end of the burnout, defined where the change in mass % reaches a steady state, defined as less than 0.05%/min.

2.5. Elemental characterization

Elemental analysis was performed using a Thermo Scientific Flash*Smart* Elemental Analyzer to quantify the CHNS/O composition of the bark/cambium samples following the flash combustion elemental analysis technique. Pulverized samples were dried at 100 °C for 24 h prior to CHNS/O analysis. The Classical Organic Elemental Analysis method, using 2,5-Bis (5-tert-butly-benzoxazol-2-yl) thiophene as the method standard, was used to test 2–4 mg of the samples (Krotz et al., n.d.). Three samples for each replicate of each bole category were analyzed, resulting in a total of nine bark/cambium replicates for each bole category.

2.6. Hydrogen pyrolysis (HyPy)

The characterization of PyC remains challenging and many thermal, chemical and optical methods have been proposed for its quantification (Sawyer et al., 2018; Mastrolonardo et al., 2017; Chang et al., 2018; Meredith et al., 2012; Haig et al., 2020). The difficulty of accurately quantifying PyC arises largely from its very definition, as the spectrum of PyC encompasses lightly charred vegetation to graphite, with carbonaceous species varying significantly in composition and environmental permanence (Schimmelpfennig and Glaser, 2011; Haig et al., 2020). Hydrogen pyrolysis (HyPy) has been shown to be a reliable method for securing the largest, most representative portion of the PyC continuum (Meredith et al., 2012; Haig et al., 2020; Ascough et al., 2009; Ascough et al., 2010). HyPy utilizes high pressure hydrogen-assisted pyrolysis with a dispersed sulphided molybdenum (Mo) catalyst to liberate labile carbonaceous species, leaving condensed, refractory carbon behind for quantification as PyC (Haig et al., 2020). Under normal pyrolysis conditions these labile species may crack and recondense onto available aromatic structures, artificially increasing the total PyC content (Preston and Schmidt, 2006). Under HyPy, the carbonaceous residue is thermally stable, highly aromatic refractory material (PyC) that has not been physiochemically altered or enhanced by the HyPy quantification technique itself and is the isolated fraction of PyC formed during the original wildfire event (Ascough et al., 2009).

Hydrogen pyrolysis (HyPy) was used to isolate the PyC fraction of the burned bark/cambium samples following the procedure developed by Meredith et al. (Meredith et al., 2012) and Ascough et al. (Ascough et al., 2009). A horizontally-oriented, 100 mm-long, 12.5 mm-diameter stainless steel reactor was constructed to house a quartz tube with an inner diameter of 3.18 mm containing unburned and burned HP and BK bark/cambium samples loaded with MoS_2 catalyst. A schematic of the HyPy reactor is shown in Fig. 2.

Ammonium tetrathiomolybdate ($(NH_4)_2MoS_4$) was combined with bark/cambium samples such that, after decomposition in the HyPy process, MoS_2 comprised 5% of the sample by weight. The bark/cambium samples were pulverized to <425 μm and loaded with the Mo catalyst precursor using a 1:1 deionized water/methanol solvent such that $(NH_4)_2MoS_4$ was 0.1 M of the aqueous solvent solution. All Mo-loaded samples were vacuum dried at 60 °C for a minimum of 24 h before subjection to the HyPy experimental procedure, and dried samples were stored under N_2 at 4 °C.

Samples were secured in the quartz tube using quartz wool on both ends, loaded into the HyPy reactor, and purged with high-pressure

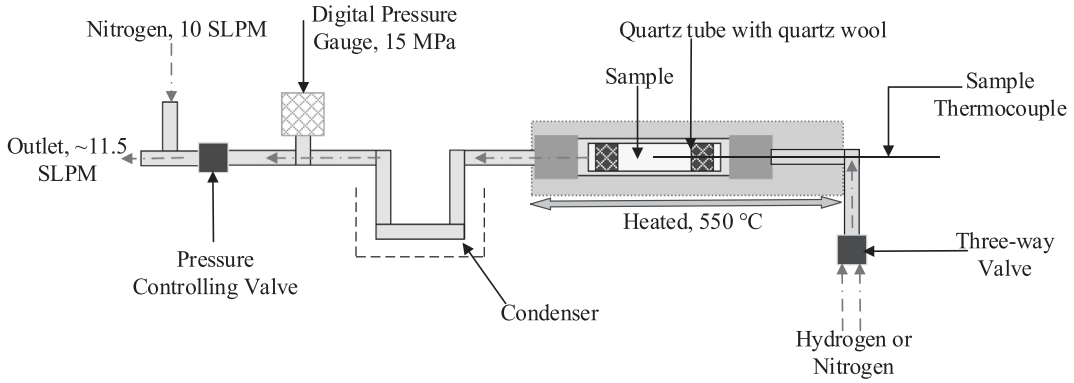

Fig. 2. Schematic of hydrogen pyrolysis (HyPy) reactor used in this study to isolate PyC.

(15 MPa), industrial grade N_2 (99.9% purity) prior to pressurizing the HyPy reactor with 99.99% purity hydrogen (H_2) at 15 MPa and at a flow rate of 1.5 SLPM. The H_2 was mixed with 10 SLPM of N_2 at atmospheric temperature and pressure prior to exiting the reactor for safety. A thermocouple inserted horizontally into the reactor monitored the sample temperature. The thermal treatment was initiated by ramping the sample temperature from 50 to 300 °C at 50 °C/min and then from 300 °C to the final temperature at 10 °C/min and held isothermal for 5 min. Meredith et al. (Meredith et al., 2012) recommended HyPy experimentation between 550 and 575 °C to capture a range of PyC residues, though additional devolatilization above 550 °C was found to be negligible in this study. Preliminary tests confirmed no significant additional loss in volatiles for HyPy trials heated to 575 °C compared to those heated to 550 °C. Thus, in this study, Mo-loaded bark/cambium samples were heated to a final isothermal temperature of 550 °C only. After the isothermal step, all samples were cooled to 100 °C in N_2 at the testing pressure. Three HyPy experimental replicates were performed for each sample and composited for further analysis.

A modified proximate analysis via TGA was used to characterize amounts of fixed carbon after HyPy treatment to investigate the effectiveness of the HyPy technique. The samples were subjected to dehydration, pyrolysis and oxidation similar to the analysis procedure outlined in Section 2.2. However, preliminary proximate analysis on HyPy-treated chars revealed negligible volatile loss above 550 °C, and, thus, the devolatilization segment of the proximate analysis was altered to mimic the HyPy experimental procedure. The HyPy chars were ramped at 100 °C/min to 300 °C and 10 °C/min to 550 °C, at which point O_2 was introduced to oxidize the remaining sample. MC, VC, FC and AC were determined for raw biomass loaded with the Mo catalyst precursor, as well as post-HyPy chars. Three repeats of each Mo-loaded bark/cambium sample and six repeats of post-HyPy samples were performed for uncertainty analysis.

Elemental analysis was performed following the procedure outlined in Section 2.5 to determine the carbon ($C_{HyPy\ char}$) content of the HyPy residue. Finally, the PyC content of the burned bark/cambium samples was determined by renormalizing the post-HyPy carbon content to the pre-HyPy mass of the bark/cambium samples using the ash content of the HyPy char ($AC_{HyPy\ char}$) obtained by the modified proximate analysis and the ash content of the pre-HyPy samples ($AC_{preHyPy}$). The renormalization relation is shown in Eq. (8):

$$PyC = C_{HyPy\ \ char} * \frac{AC_{preHyPy}}{AC_{HyPy\ \ char}} * 100\ [\%] \tag{8}$$

HyPy of the unburned BK and HP bark/cambium samples should produce no PyC because those samples underwent no charring in the fire event. The results of HyPy characterization of the unburned HP and BK in this study, although quite low, were not zero. These residues are artifacts of the organic aromatic ring structures within the unburned biomass. Therefore, the actual PyC contents of the burned HP and BK were determined by deducting the apparent PyC found from their unburned bark/cambium sample counterparts.

2.7. Carbon partitioning and net heat output

The results of the bark/cambium HyPy PyC characterization and elemental analyses were used to assess carbon partitioning between carbon lost from the site of the Badger Creek Fire via pyrolysis and char oxidation, and carbon retained at the site in the forms of unaffected and charred biomass. Average bark/cambium thicknesses, based on eight thickness measurements made at 45° increments around the circumference of each bole type, were used to determine the volume of bark and cambium per unit length of bole based on a bole cross-sectional area that was 16.5 cm in diameter at the inside surface of the bark/cambium. The total carbon content of the bark/cambium layer of a bole per meter length (CPL_i) was calculated by

$$CPL_i = \pi\left((r_o + t_i)^2 - r_o^2\right) * \rho_i * X_{C,i}\ \left[\frac{g\ C}{m\ bole}\right] \tag{9}$$

for burned and unburned HP and BK, where $\pi((r_o + t_i)^2 - r_o^2)$ is the cross-sectional area of the bark/cambium layer for bole type i, where i indicates burned or unburned HP or BK. The inner radius, r_o, is half the 16.5 cm diameter for each bole, while the thickness, t_i, is the unique average measured bark/cambium thickness for each bole type. The bark/cambium density, ρ_i, was determined by massing bark/cambium samples for each bole type and using t_i along with sample area, measured using ImageJ (Rasband, n.d.), to determine particle volume. The mass fraction of elemental carbon within a given bole type, $X_{C,i}$, was acquired by elemental analysis. Carbon released from HP or BK boles due to fire was then determined by differences in CPL_i between unburned and burned samples. The total PyC content of the bark/cambium layer for each bole type per meter length, $PyCPL_i$, was calculated using Eq. (9) by replacing $X_{C,i}$ with $X_{PyC,i}$, where $X_{PyC,i}$ was determined as outlined in Section 2.6. Volatile content of the bark/cambium per meter length, $VCPL_i$, was likewise calculated by replacing $X_{C,i}$ with $X_{VC,i}$.

The chemical energy in the bark/cambium layer per unit length of the uniform size boles, EPL_i with units of kJ/(m of bole length), can also be calculated using a variant of Eq. (9) by replacing $X_{C,i}$ with the measured higher heating value, HHV_i. Heating value analyses of burned and unburned HP and BK bark/cambium were performed by Wyoming Analytical Laboratories in Laramie, WY, USA. Again, by difference, the energy released per meter length can be determined between burned and unburned boles. Measured and calculated values of $X_{C,i}$, ρ_i, HHV_i, CPL_i, $PyCPL_i$, and EPL_i are all on a DAF basis.

Lastly, the results were scaled up to the area impacted by the Badger Creek Fire to estimate total carbon emissions and total energy released, as well as total PyC produced as a result of this fire, and to assess full-scale impacts of bark beetle mortality on these quantities. Most recently in 2017, fourteen plots of 150 m^2 in the Chimney Park area of the Medicine Bow-Routt NF were field tested to assess bark beetle mortality. The average basal area of lodgepole pine within these plots was 13 m^2/ha, with 58% of the basal area determined as beetle-killed before the Badger Creek Fire. For an average diameter of 16.5 cm at a height of 1.0 m, a homogenous age class of trees will have an average height from base to top of crown of 12.5 m (Kayes and Tinker, 2012; Reed et al., 2014). In the scale-up calculations performed in this study, the simplifying assumption was made that the charring characteristics, including char depth and composition, at 1.0 m height were representative of all heights along the bole. These details of the fire-affected area were used in conjunction with the experimental characterization of the boles performed in this study to scale up the carbon partitioning for the entire 21,310 acres of the Badger Creek Fire.

3. Results and discussion

3.1. Characterization of charring extent

Proximate analyses of FC and VC in the bark/cambium, sapwood and heartwood layers of the burned and unburned HP and BK boles are shown in Fig. 3a on a DAF basis. Spatially resolved particle samples revealed that the FC and VC did not vary significantly with radius within either the sapwood or heartwood layers. Furthermore, no significant differences in FC or VC were observed between the burned and unburned sapwood and heartwood layers for HP or BK, or between the burned and unburned HP bark/cambium. In contrast, the BK bark/cambium layers showed evidence of significant charring by increased FC and decreased VC measured in the burned BK as compared to the unburned BK. In summary, the proximate analysis results suggested that carbonization, and therefore PyC production, was limited to the bark/cambium layers of the boles and was more prominent in BK than HP. As a result of these findings, further characterization was limited to the bark/cambium layers only. Proximate analysis TGA mass loss profiles of solely the bark/cambium are shown in Fig. 3b and further illustrate the differences summarized in Fig. 3a. The drying step occurs first with a dwell time of 10 min at 100 °C and ends at approximately 15 min when the temperature begins ramping from 100 °C. Pyrolysis is the extensive mass loss event occurring immediately following drying from 15 to 42 min or from 100 to 950 °C. Following pyrolysis, the sample is cooled to 750 °C before an air environment is introduced to initiate oxidation. Oxidation can be identified as the rapid mass loss event beginning at approximately 49 min.

Compositional changes to the bark/cambium layers were further examined qualitatively via scanning electron microscopy (SEM), and SEM images of unburned and burned HP and BK bark/cambium layers are shown in Fig. 4. Fig. 4a, c, e and g show impacts of the bark beetle and fire on the bark side of the bark/cambium layer. Fig. 4b, d, f and h show impacts on the cambium side. Beetle impacts can be observed in the structural degradation between unburned HP and BK in the cambium (Fig. 4b and f), and particularly in the bark (Fig. 4a and e). The bark of HP underwent some deterioration of fiber assembly due to light charring from fire, observable in Fig. 4c. In contrast, images of unburned and burned HP cambium (Fig. 4b and d, respectively) show that the cambium remained relatively intact after the fire. Between the unburned and burned BK, however, distinct changes in structure and arrangement of the fibers can be observed, suggesting degradation of those fibers and charring from the exterior bark (Fig. 4e and g) through to the cambium (Fig. 4f and h). These SEM imaging results are consistent with macroscopic visual observations (Fig. 1b and c) and proximate analysis results (Fig. 3) indicating that charring extended through the entire bark/cambium layer of burned BK, while

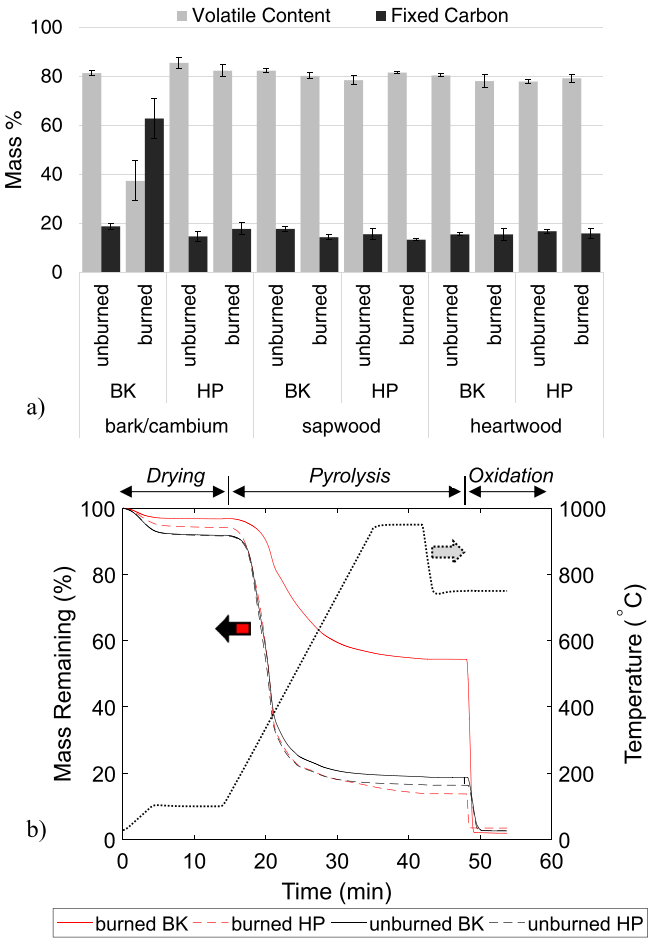

Fig. 3. Proximate analysis results showing a) volatile and fixed carbon contents on a DAF basis of burned and unburned BK and HP for bark/cambium, sapwood and heartwood layers, and b) mass loss profiles of burned and unburned BK and HP bark/cambium during drying, pyrolysis and oxidation.

the charring depth was significantly less in burned HP. These results suggest that pre-fire disturbance from the bark beetle led to reduction in the fire resistivity of the protective bark/cambium in affected trees.

Additional insights into the differences in charring extent and depth in HP and BK were sought by measuring bark/cambium layer thicknesses. The influence of bark thickness on fire resistivity has been established by a number of studies (Hengst and Gretel, 1994; Lawes and Richards, 2011; Pinard and Huffman, 1997). Generally, the bark thickness is considered to be a significant determining factor in predicting survival and recovery of the vascular cambium from fires. Bark/cambium thicknesses were measured to be 2.10 ± 0.58, 2.02 ± 0.50, 1.87 ± 0.22, and 2.28 ± 0.33 mm for burned and unburned BK and burned and unburned HP, respectively. There is no statistical difference between these thicknesses and, thus, the relative thicknesses of the bark/cambium layers alone do not explain the observed differences in charring between HP and BK.

3.2. Kinetic parameters

Fig. 5a and b show isoconversional ln β vs. 1000/T lines from the pyrolysis of unburned BK and HP, respectively, for the five investigated heating rates. The R^2 values for each isoconversional linear regression are summarized in Table 1. Pyrolysis kinetics above 80% conversion were not assessed due to inconsistencies in the linear fits and, thus, inaccurate kinetic parameter values that would be derived from these fits. Notably, kinetic parameters were derived in this study over a range of

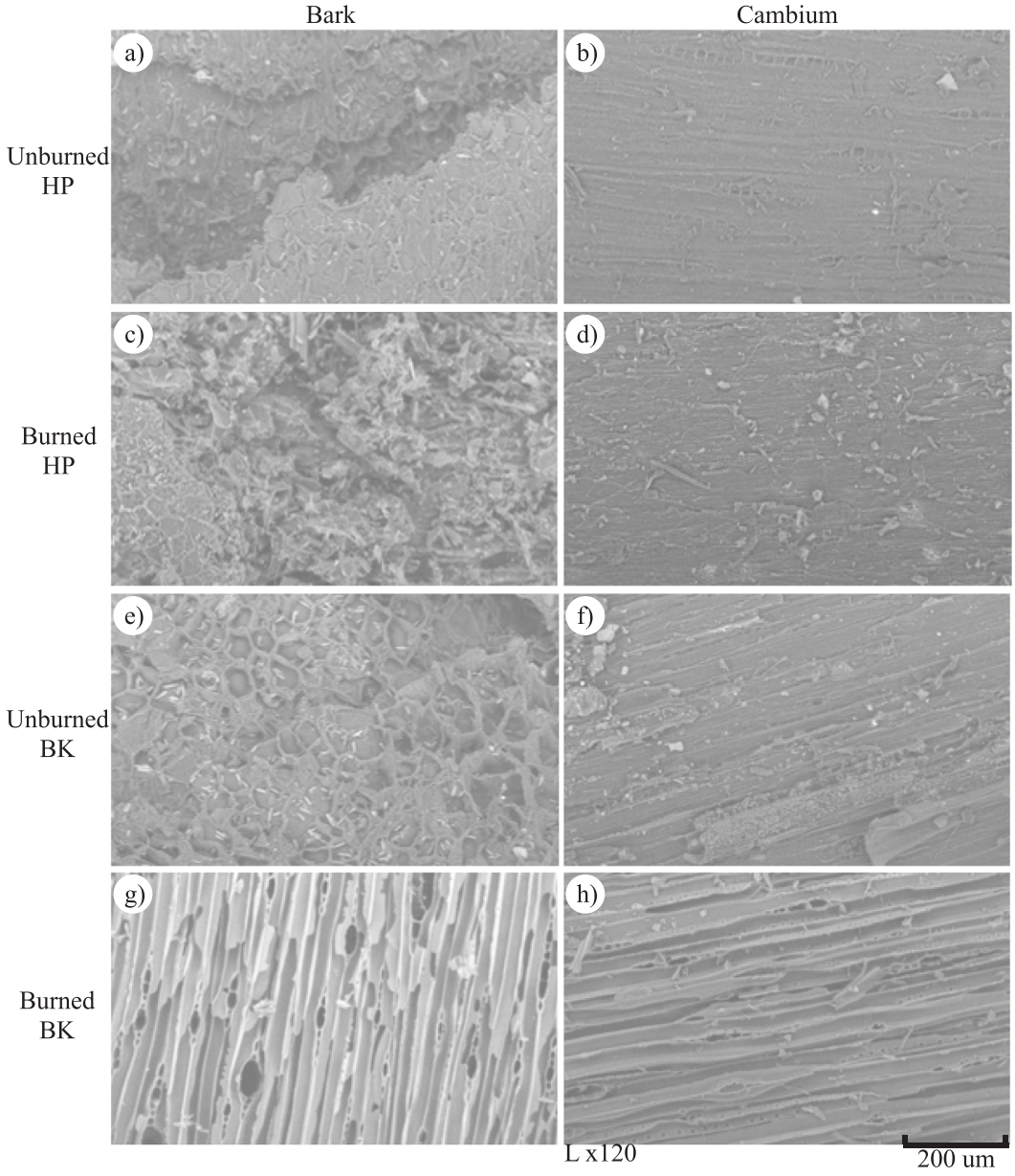

Fig. 4. SEM images of unburned HP a) bark and b) cambium; burned HP c) bark and d) cambium; unburned BK e) bark and f) cambium; and burned BK g) bark and h) cambium.

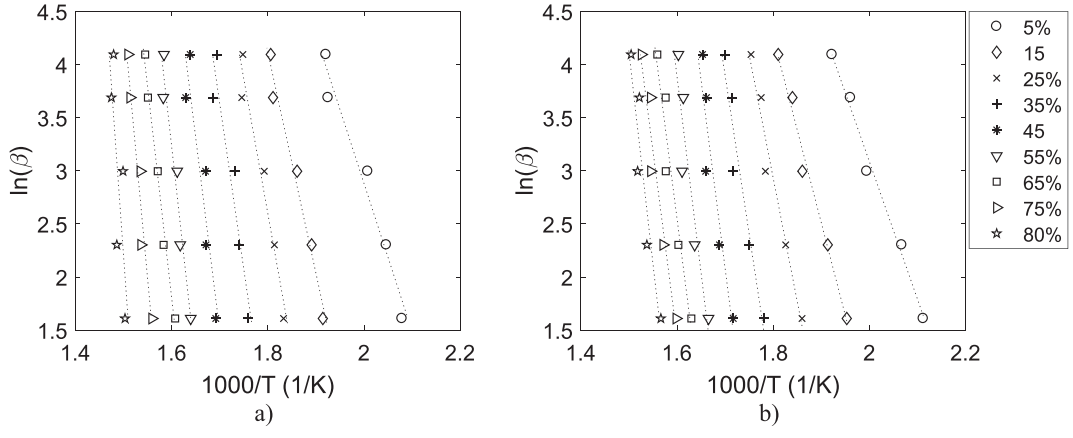

Fig. 5. Isoconversional lines for the pyrolysis of unburned a) BK and b) HP.

Table 1
R^2 values for linear regressions of isoconversional extents (α) from 5 to 80%.

R^2									
α	5%	15%	25%	35%	45%	55%	65%	75%	80%
BK	0.963	0.976	0.954	0.903	0.865	0.950	0.987	0.957	0.594
HP	0.990	0.985	0.965	0.924	0.877	0.877	0.931	0.934	0.876

heating rates from 5 to 60 °C/min, which is a larger range and higher heating rates than are typically utilized in OWF kinetic parameter derivations, but those higher heating rates generally showed no detrimental effect on R^2 values. Table 1 shows that the poorest linear fit over this wide range of heating rates is at the highest extent of conversion (α = 80%).

The activation energies and pre-exponential factors as functions of conversion extent, derived using results shown in Fig. 5 and the OWF model, are presented in Fig. 6. Arenas et al. (Arenas et al., 2019) reported activation energy values as high as 400 kJ/kg at 90% conversion for pinewood using several isoconversional methods. Those authors also listed activation energies for orange peel, a fruit protective structure, of approximately 550 kJ/kg at the same conversion extent. The high E_a for both BK and HP reported in the present study, up to 503 and 315 kJ/mol, respectively, likely result from the high lignin content present in plant structural materials such as bark and which is recalcitrant to degradation (Srivastava, n.d.). BK and HP display some differences in kinetic behavior, suggesting variation in the decomposition mechanism of each bark/cambium type. BK and HP kinetic parameters are observed to increase similarly and nearly linearly to approximately 45% conversion, beyond which differences between the two feedstocks cause the kinetic behavior to deviate significantly. The activation energies and pre-exponential factors of BK are higher than those of HP above approximately 50% conversion. These differences in kinetic parameters between HP and BK indicate less heating needed for significant reactions to occur in HP. The pyrolysis kinetic behavior mimics that observed in Fig. 3b where the pyrolysis mass loss behaviors of unburned HP and BK are identical up to approximately 390 °C (~50% conversion), after which BK devolatilization slows and mass loss becomes less susceptible to heating until oxidation. These results, taken together with the reduced charring of HP, suggest a protective effect from the presence of labile volatile species. The higher kinetic parameters of BK indicate that a significant portion of the volatile barrier against charring had already been removed over the course of beetle infestation and induced mortality. More energy, in the form of even greater pyrolysis temperatures, is then needed to continue degradation of the remaining recalcitrant components of the bark/cambium in the BK. This also indicates that BK would be more susceptible to charring as a significant component of fire resistivity in healthy pine – volatile bark/cambium content – is missing.

3.3. Ignition temperature and char oxidation rate

The Stage 1, homogeneous gas-phase ignition temperatures of HP and BK bark/cambium were 313 ± 3.0 °C and 302 ± 3.1 °C, respectively. The Stage 2, heterogeneous solid char ignition temperatures were 414 ± 2.9 °C and 392 ± 7.7 °C, respectively. The oxidation rates of the HP and BK chars during Stage 2 oxidation were 20.1 ± 1.4 %/min and 21.3 ± 3.3 %/min, indicating that once the volatile component of the bark/cambium had been extirpated, the char burnout behavior was similar between BK and HP. The ignition temperatures, volatile contents and kinetic parameters suggest that, while the volatile content of unburned HP was only slightly higher than that of unburned BK (Fig. 3), the loss of volatiles in the BK bark/cambium due to the bark beetle disturbance corresponded to considerably increased vulnerability to charring during wildfire as indicated by the kinetic analysis and lower ignition temperatures of BK. Considering the rapid and relatively short duration of the heating experienced by vegetation during wildfire, these results help explain the greater extent of BK charring as compared to HP during the Badger Creek Fire and suggest more extensive PyC formation from BK.

3.4. PyC characterization

Proximate analysis mass loss profiles and results for chars created using the HyPy technique to isolate the PyC component of burned BK and HP are shown in Fig. 7. First, Fig. 7a illustrates the effectiveness of the HyPy technique for isolating and accurately quantifying PyC in organic samples. HP that had not undergone HyPy was pyrolyzed in N_2 by heating samples to 700 °C at 40 °C/min and holding them isothermal for 20 min in the TGA. The pyrolyzed samples were then subjected to the same modified proximate analysis underwent by all post-HyPy char samples. Fig. 7a compares the proximate analysis profiles of N_2-pyrolyzed HP char and the post-HyPy HP char. Since minimal mass loss occurred at temperatures below 300 °C, the mass loss profiles were truncated to show the 10 °C/min pyrolysis step starting from 300 °C and the oxidation step of the proximate method for better visualization. Comparing to the proximate mass loss shown in Fig. 3b, only pyrolysis and oxidation are shown in Fig. 7a. Pyrolysis mass loss occurred first until approximately 28 min, at which point the sample was subjected to an air environment. The rapid mass loss event at approximately 30 min was the start of the combustion or char burnout step. The results shown here are strikingly different from those shown in Fig. 3b for raw biomass samples. In Fig. 7a, the samples had already

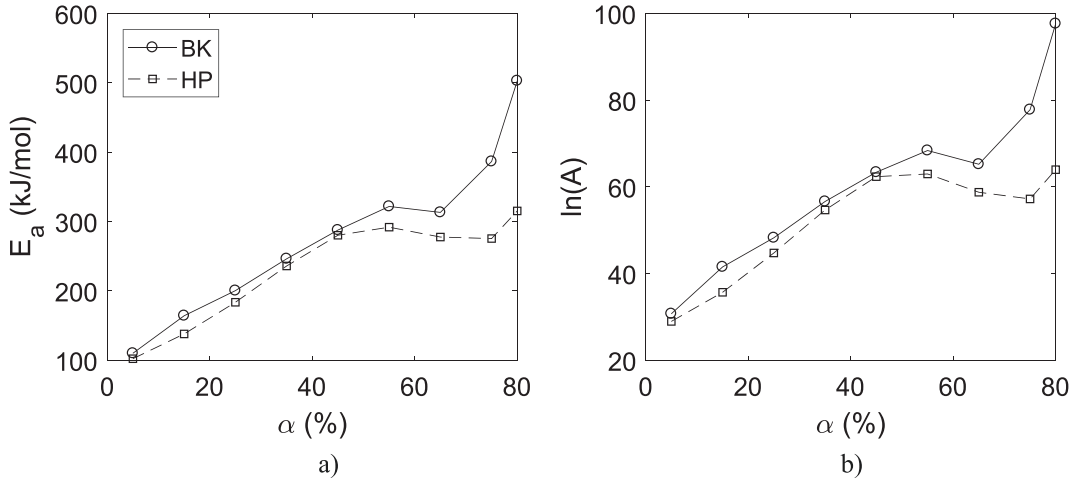

Fig. 6. a) Activation energies and b) pre-exponential factors of BK and HP pyrolysis as functions of conversion extent (α), obtained using the OWF isoconversional method.

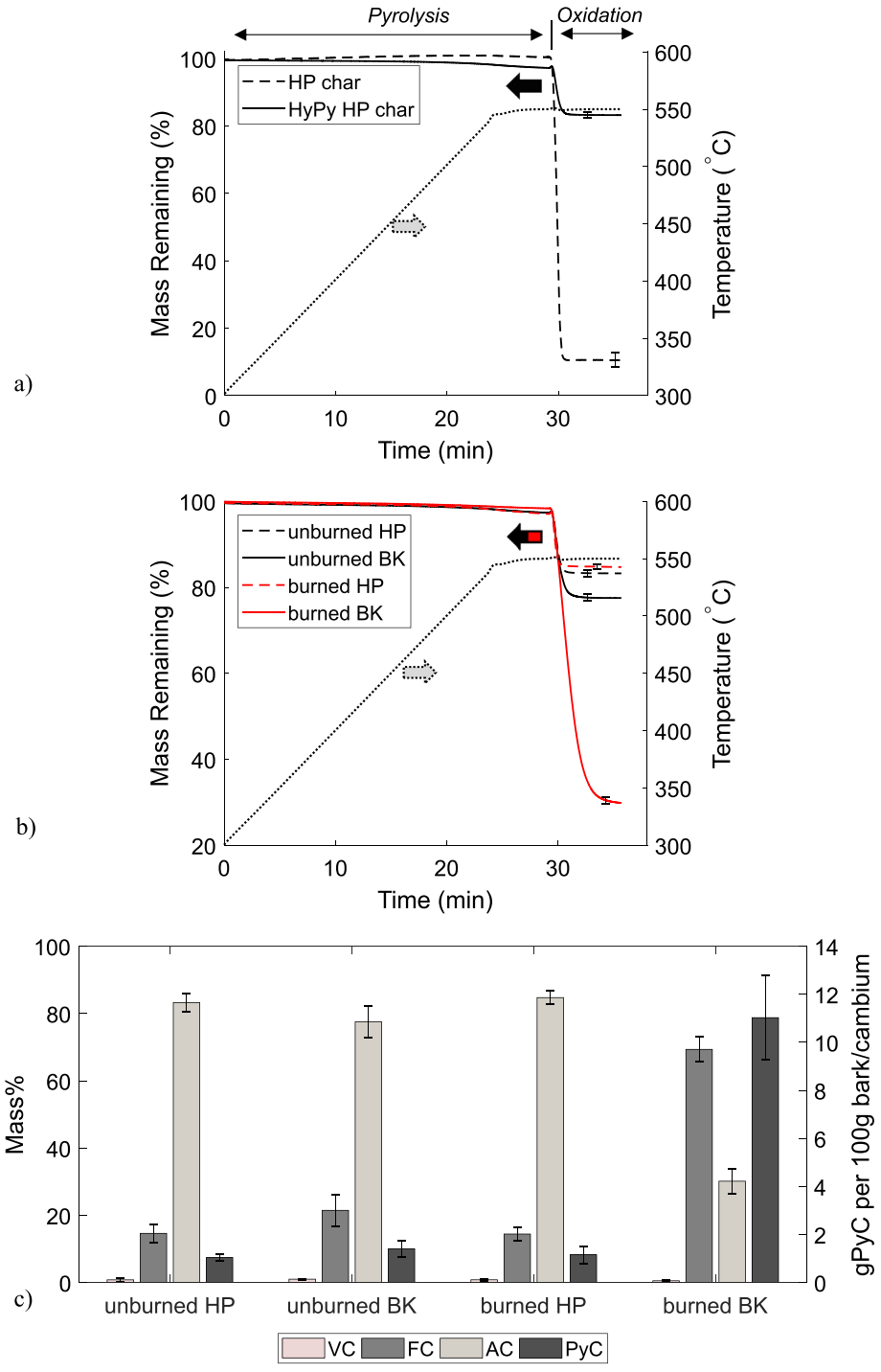

Fig. 7. a) TGA mass loss profiles demonstrating the effectiveness of the HyPy technique for isolating PyC, b) proximate analysis mass loss profiles of the post-HyPy bark/cambium samples, and c) volatile (VC), fixed carbon (FC) and ash (AC) contents (mass %, dry basis) from proximate analysis of post-HyPy bark/cambium samples, as well as calculated PyC content of unburned and burned BK and HP (g of PyC per 100 g of bark/cambium sample on a DAF basis).

undergone extensive pyrolysis and charring, losing a significant fraction of their volatile content. Results show substantially more fixed carbon in the non-HyPy HP char than the HyPy char due to the formation of PyC under pyrolysis in N_2, highlighting the need for the HyPy technique to isolate PyC in burned biomass samples. Proximate analyses of post-HyPy unburned and burned HP and BK chars are compared in Fig. 7b. The proximate analysis results for the HyPy chars (dry basis) and the PyC content of the feedstocks (DAF basis), calculated from the post-HyPy carbon content and renormalized to the pre-HyPy sample mass using Eq. (8), are provided in Fig. 7c. Carbon contents of post-HyPy chars obtained via elemental analysis were 60.2 ± 4.2% and 18.1 ± 4.2% for burned and unburned BK, respectively, and 11.8 ± 2.5% and 13.0 ± 1.8% for burned and unburned HP, respectively, on a dry basis. Ash content accounted for a significant portion of the HyPy char compositions due to the extensive removal of labile material during HyPy, resulting in a sample that was primarily ash and PyC.

Notably, the unburned BK and HP samples showed small amounts of PyC content which indicates that some PyC was formed during HyPy. This PyC formation is due to generation of pyrolysis char from residual organic structures in the original raw biomass and some formation

during HyPy is likely unavoidable. Nevertheless, results can be analyzed by difference, comparing the PyC contents of burned feedstocks against those of their unburned counterparts, where the latter serve as a baseline. The PyC contents of unburned and burned HP were 1.04 and 1.16 ± 0.3 gPyC per 100 g of feedstock, respectively, suggesting minimal PyC formation in burned HP and resistance of HP bark/cambium to charring in wildfire. In contrast, burned BK contained significantly more PyC than its unburned counterpart at 1.40 and 11.0 ± 1.0 gPyC per 100 g of feedstock for unburned and burned BK, respectively. These results correspond to the production of PyC in HP and BK bark/cambium after wildfire of 0.12 ± 0.4 and 9.62 ± 1.8 gPyC per 100 g of bark/cambium, respectively. This 80 times greater PyC content in BK bark/cambium confirms the enhancement of carbonization of BK over HP that has been indicated by other results presented in this study.

3.5. Carbon and PyC partitioning

The PyC results obtained from HyPy analysis were used to estimate the total PyC produced for the Badger Creek Fire impacted area. Table 2 summarizes the bark/cambium densities, elemental carbon contents, carbon per meter length of bole, PyC per meter length of bole, and volatile content per meter length of bole of the bark/cambium feedstocks. Also shown in Table 2 are the estimated total and per hectare carbon, PyC and volatile contents for the impacted fire region. Due to the lack of statistical difference in burned and unburned bark/cambium thicknesses, average thicknesses of 1.96 mm and 1.94 mm were used for BK and HP, respectively, to calculate the results in Table 2.

The ramifications of the loss of the volatile protective barrier in BK is emphasized by the bark/cambium density measurements in Table 2, where the density of unburned BK is significantly less than that of unburned HP and, while both feedstocks show a decrease in density after burning, the BK is more dramatically reduced. These density values give insight into bark/cambium fire resistivity, as the larger volatile content of healthy bark and cambium can include components that help resist thermal degradation, such as sap, but these components are reduced when a tree dies, lowering bark/cambium density (Santín et al., 2017; Pérez-Ramirez et al., 2012). Analysis of the density, volatile contents, ignition temperatures and kinetic parameters suggests an explanation for the enhancement of char formation in burned BK. Though the loss of volatiles in unburned BK as compared to unburned HP is small (Fig. 3), significant damage is dealt to the bark/cambium protective barrier. The cost of the impacts of the bark beetle become quite apparent with the 11 and 22 °C decrease in ignition temperatures of BK during Stage 1 and Stage 2 combustion, respectively. Furthermore, the increase in kinetic parameters of BK at high extents of conversion indicate that the more recalcitrant species to pyrolysis have already been lost in BK. The deterioration of the protective bark/cambium from beetle impacts is then fully realized by the significant enhancement of carbon and, ultimately, PyC in burned BK observed visually and quantitatively confirmed in this work.

The total amounts of elemental carbon for each bole type show that unburned HP had greater elemental carbon than unburned BK (Table 2). This results from not only a higher elemental carbon fraction in unburned HP as compared to unburned BK, but also from greater bark/cambium densities (Lawes and Richards, 2011). Regarding the carbon remaining in situ after the fire, only 0.15% of the carbon retained in burned HP bark/cambium was PyC. This corresponds to a calculated 0.015 GgPyC (1.73 kgPyC/ha) left onsite from burning of HP. Conversely, 11.6% of the carbon retained in burned BK bark/cambium was PyC, leaving a calculated 0.70 GgPyC (80.8 kgPyC/ha) onsite after the fire. Lastly, the total carbon calculated to have been released during the fire event in the form of volatiles and oxidized char was 6.6 and 1.3 GgC (764 and 143 kgC/ha) from BK and HP, respectively, resulting in a total carbon release from lodgepole pine tree boles as a result of the Badger Creek Fire of 7.9 GgC (907 kgC/ha) or about 0.0004% of the estimated annual global release of carbon from wildfires. The total PyC generated in tree boles by the Badger Creek Fire (calculated to be 0.71 GgPyC or 82.5 kgPyC/ha) corresponds to 0.0002–0.0006% of the annual global PyC production of 116–385 TgPyC estimated by Santín et al. (Santín et al., 2016).

For comparison, if the total burned area consisted solely of healthy lodgepole pines prior to the fire, the theoretical total carbon released as volatiles and oxidized char, and the total PyC retained in situ after wildfire would be 3.0 GgC (340 kgC/ha) and 0.036 GgPyC (4.12 kgPyC/ha), respectively. Thus, the theoretical carbon released and PyC formed due to beetle infestation and consequent mortality was increased by an additional 4.9 GgC (567 kgC/ha) and 0.67 GgPyC (78.4 kgPyC/ha), respectively. These results have significant implications for the carbon stored in PyC and the carbon released from wildfires in beetle-impacted lodgepole pine forest ecosystems, and for global carbon estimates.

3.6. Net heat output

The higher heating values of the bark/cambium and the released volatiles between unburned and burned boles, chemical energy per meter length (EPL_i) of the bark/cambium layers, and total heat contents and output are shown in Table 3.

The results of the heating value and energy analyses were used to estimate the total heat released by volatile combustion during the fire, which was equivalent to 170 TJ for BK and 79.9 TJ for HP, or an estimated total heat release of 250 TJ due to the Badger Creek Fire. Verón et al. (2012) reported an estimated global energy release from fires of 8300 ± 592 PJ per year from a land area of 3.3 to 4.3 million km^2. For the Badger Creek Fire burned area of 86.2 km^2, this would correspond to an energy release of approximately 220 TJ, demonstrating remarkable agreement with the scale-up energy analysis performed in this study. Alternatively, for a healthy lodgepole pine ecosystem, the total heat released during wildfire would be approximately 190 TJ, corresponding to an intensification of heat released during fire due to bark beetle-induced mortality by 60 TJ.

Table 2
Bark/cambium densities, elemental carbon contents, carbon per length (CPL), PyC per length (PyCPL), and volatile content per length (VCPL) are presented. Estimated total and per-hectare carbon, PyC and volatile contents derived for burned and unburned BK and HP bark/cambium over the impacted area of the Badger Creek Fire are also presented. Results are reported on a DAF basis.

	Density (kg/m^3)	%C	CPL (gC/m)	Total C (GgC) *(kg/ha)*	PyCPL (gPyC/m)	Total PyC (GgPyC) *(kg/ha)*	VCPL (gVC/m)	Total VC (GgVC) *(kg/ha)*
BK								
Unburned	500 ± 27	64.4 ± 6.5	331 ± 34	12.6 ± 1.1 *1459 ± 130*	–	–	418 ± 26	15.9 ± 0.8 *1843 ± 94*
Burned	185	82.8	158	6.0 *695*	18.3 ± 2.8	0.70 ± 0.1 *80.8 ± 5.6*	70.9	2.70 *313*
HP								
Unburned	583	67.0	398	11.0 *1271*	–	–	508	14.0 *2240*
Burned	470	73.7	353	9.7 *1128*	0.54	0.015 *1.73*	408	11.2 *1800*

Table 3
HHV_i and EPL_i results for unburned and burned BK and HP bole bark/cambium, and total heat contents and output.

	HHV_i (kJ/kg)	EPL_i (kJ/m)	Total energy content of bark/cambium (TJ)	Total energy released (TJ)	HHV_i of volatiles released (kJ/kg)
BK					
Unburned	19,990	10,280 ± 591	391 ± 19	–	–
Burned	30,530	5812	221	170 ± 27	13,800 ± 6200
HP					
Unburned	23,780	14,140	389	–	–
Burned	24,220	11,530	309	79.9	25,230

The heating value energy contents of the unburned tree bark/cambium for the entire Badger Creek area were estimated to be 391 and 389 ± 19 GJ for BK and HP, respectively. Based on energy released and mass lost, an average HHV of volatiles released during HP combustion was found to be 25,200 kJ/kg, and an average HHV for volatiles released during BK combustion was 13,900 kJ/kg. These heating values encompass a larger range than the heating values of simple gas mixtures typically considered representative of homogeneous gas-phase combustion in literature (Pérez-Ramirez et al., 2012). The heating values presented in this work may therefore help improve the accuracy of beetle-impacted forest fire models.

4. Conclusions

Prediction and modeling of wildland fire are confounded by highly variable fuel compositions, loads and fire conditions. This study aimed to enhance modeling efforts by assessing how an ecosystem disturbance due to beetle infestation might alter fire dynamics and carbon partitioning. In this work, the properties of unburned and burned bark beetle-killed and healthy lodgepole pine were investigated using unique field data from the 2018 Badger Creek Fire in southeastern WY, USA, to assess the impacts of the bark beetle infestation and induced mortality on charring extent, carbon loss, heat output and PyC production. Disturbance by bark beetle was shown to change the bark/cambium structure and composition and, therefore, the fuel characteristics and combustion behavior of lodgepole pine, but these impacts generally did not extend past the bark/cambium layer. Bark/cambium volatile content, kinetic parameters, ignition temperature and density were used to identify a greater fire resistivity in HP bark/cambium over BK, which led to measured increases in PyC contents in burned BK over HP. Uniform bole sizes were used to compare carbon, PyC and energy partitioning between burned and unburned samples and to clarify unique characteristics between healthy and beetle-killed pine that led to significant differences in final charring extents. Heating values of volatiles emitted from burned and unburned boles were also estimated and further confirmed that the change in fuel composition due to the bark beetle resulted in a change in fire behavior and products.

Carbon partitioning and energy released were scaled up to estimate the impacts over the entire Badger Creek fire area. The total amount of carbon released to the atmosphere from lodgepole pine tree boles in the Badger Creek Fire was estimated to be 7.9 GgC (907 kgC/ha) and the total amount of PyC formed and retained was estimated to be 0.71 GgPyC (82.5 kgPyC/ha). The total energy released by the fire was estimated as 250 TJ. Scale-up analyses were also performed for a hypothetical healthy lodgepole forest ecosystem of the same total burned area to assess the net impacts of the bark beetle on combustion products. In a hypothetical equivalent healthy forest ecosystem, the theoretical total carbon released as volatiles was estimated to be 3.0 GgC (340 kgC/ha), total PyC onsite was calculated to be 0.036 GgPyC (4.12 kgPyC/ha) and the net heat output was estimated to be 190 TJ. Thus, these combustion products were significantly enhanced in the actual, beetle-disturbed ecosystem. The 58% tree mortality resulted in 32% greater fire heat output and more extensive burning and charring, with almost 3 times more carbon released to the atmosphere and nearly 20 times more carbon formed into PyC. While the conclusions drawn in this study are based on the boles of one vegetation type burned during one unique wildfire incident, significant impacts of beetle disturbance are elucidated. The differences in carbon stocks and heat output after wildfire due to the bark beetle epidemic found in this study improve estimates for fire behavior models and global carbon accounting, and support a need for larger-scale ecological studies in fire- and insect-impacted ecosystems.

CRediT authorship contribution statement

Alexandra Howell: Conceptualization, Methodology, Experimentation, Data analysis, Writing.

Dr. Mario Bretfeld: Ecological data, Manuscript review.

Dr. Erica Belmont: Conceptualization, Methodology, Data analysis, Writing, Supervision.

Declaration of competing interest

The authors declare that they have no known competing financial interests or personal relationships that could have appeared to influence the work reported in this paper.

Acknowledgements

This research was supported by the National Science Foundation award nos. 1847498 and 1904421. The authors also recognize the support of the Ecology & Biogeochemistry CORE and the Robert A. Jenkins Microscopy Laboratories at the University of Wyoming under NSF grant no. 1655726 and the Wyoming Sensory COBRE award (no. P20GM121310) from the National Institute of General Medical Sciences, respectively.

References

Albini, F.A., 1976. Estimating Wildfire Behavior and Effects: General Technical Report INT-30. Intermountain Forest and Range Experiment Station.

Albini, F.A., 1980. Thermochemical properties of flame gases from fine wildland fuels. USDA For. Serv. Res. Pap. INT-243.

Alexander, M.E., Cruz, M.G., 2013. Are the applications of wildland fire behaviour models getting ahead of their evaluation again? Environ. Model. Softw. 41, 65–71.

Arenas, C.N., Navarro, M.V., Martinez, J.D., 2019. Pyrolysis kinetics of biomass wastes using isoconversional methods and the distributed activation energy model. Bioresour. Technol. 288.

Ascough, P.L., et al., 2009. Hydropyrolysis as a new tool for radiocarbon pre-treatment and the quantification of black carbon. Quat. Geochronol. 4, 140–147.

Ascough, D.C., Bird, P.L., Meredith, M.I., Wood, W., Snape, R.E., Brock, C.E., Higham, F., Large, T.F.G., Apperley, D.J., 2010. Hydropyrolysis: implications for radiocarbon pre-treatment and characterization of black carbon. Radiocarbon 52 (2), 1336–1350.

Badger Creek Fire. Incident Information System [Online]. Available. https://inciweb.nwcg.gov/incident/5836/.

Berner, J.A., Logan, T., Law, Law, Beverly E., Meddens, Arjan, J.H., Hicke, 2012. Tree mortality from fires, bark beetles, and timber harvest during a hot and dry decade in the western United States (2003–2012). Environ. Res. Lett. 12, 1–13.

Bond, M.L., Lee, D.E., Bradley, C.M., Hanson, C.T., 2009. Influence of pre-fire tree mortality on fire severity in conifer forests of the San Bernardino Mountains, California. Open For. Sci. J. 2, 41–47.

Chang, Z., et al., 2018. Benzene polycarboxylic acid — a useful marker for condensed organic matter, but not for only pyrogenic black carbon. Sci. Total Environ. 626, 660–667.

Chatterjee, S., Santos, F., Abiven, S., Itin, B., Stark, R.E., Bird, J.A., 2012. Elucidating the chemical structure of pyrogenic organic matter by combining magnetic resonance, mid-infrared spectroscopy and mass spectrometry. Org. Geochem. 51, 35–44.
Donato, D.C., Campbell, J.L., Fontaine, J.B., Law, B.E., 2009. Quantifying char in postfire woody detritus inventories. Fire Ecol. 5 (2), 104–115.
Edburg, S.L., et al., 2012. Cascading impacts of bark beetle-caused tree mortality on coupled biogeophysical and biogeochemical processes. Front. Ecol. Environ. 10 (8), 416–424.
Frankman, David, Webb, Brent W., Bulter, Bret W., Jimenez, Daniel, Forthofer, Jason M., Sopko, Paul, Shannon, Kyle S., Hiers, J. Kevin, Ottmar, R.D., 2012. Measurements of convective and radiative heating in wildland fires. Int. J. Wildl. Fire 22, 157–167.
Gale, N.V., Thomas, S.C., 2019. Dose-dependence of growth and ecophysiological responses of plants to biochar. Sci. Total Environ. 658, 1344–1354.
García, R., Pizarro, C., Lavín, A.G., Bueno, J.L., 2013. Biomass proximate analysis using thermogravimetry. Bioresour. Technol. 139, 1–4.
Goldberg, E.D., 1985. Black Carbon in the Environment: Properties and Distribution.
Haig, J., Bird, M.I., Ascough, P.L., Wurster, C.M., 2020. A rapid throughput technique to isolate pyrogenic carbon by hydrogen pyrolysis for stable isotope and radiocarbon analysis. Rapid Commun. Mass Spectrom. 34, 1–11.
Harvey, B.J., Donato, D.C., Turner, M.G., 2014. Recent mountain pine beetle outbreaks, wildfire severity, and postfire tree regeneration in the US Northern Rockies. Proc. Natl. Acad. Sci. 111 (42).
Hengst, J.O., Gretel, E., Dawson, 1994. Bark properties and fire resistance of selected tree species from the central hardwood region of North America. Can. J. For. Res. 24 (4), 688–696.
Hobley, E.U., Le Gay Brereton, A.J., Wilson, B., 2017. Forest burning affects quality and quantity of soil organic matter. Sci. Total Environ. 575, 41–49.
Jenkins, M.J., Hebertson, E., Page, W., Jorgensen, C.A., 2008. Bark beetles, fuels, fires and implications for forest management in the Intermountain West. For. Ecol. Manag. 254, 16–34.
Jenkins, M.J., Runyon, J.B., Fettig, C.J., Page, W.G., Bentz, B.J., 2014. Interactions among the mountain pine beetle, fires, and fuels. For. Sci. 60 (3), 489–501.
Jones, M.W., Santín, C., Van Der Werf, G.R., Doerr, S.H., 2019. Global fire emissions buffered by the production of pyrogenic carbon. Nat. Geosci. 12.
Kayes, L.J., Tinker, D.B., 2012. Forest structure and regeneration following a mountain pine beetle epidemic in southeastern Wyoming. For. Ecol. Manag. 263, 57–66.
Keeley, J.E., 2009. Fire intensity, fire severity and burn severity: a brief review and suggested usage. Int. J. Wildl. Fire 18, 116–126.
Kipfmueller, K.F., Baker, W.L., 2000. A fire history of a subalpine forest in south-eastern Wyoming, USA. J. Biogeogr. 71–85.
Klutsch, J.G., et al., 2009. Stand characteristics and downed woody debris accumulations associated with a mountain pine beetle (Dendroctonus ponderosae Hopkins) outbreak in Colorado. For. Ecol. Manag. 258 (5), 641–649.
Knicker, H., Hilscher, A., González-vila, F.J., Almendros, G., 2008. A new conceptual model for the structural properties of char produced during vegetation fires. Org. Geochem. 39, 935–939.
L. Krotz, F. Leone, and G. Giazzi, "Thermo Scientific Flash Smart Elemental Analyzer: Fully Automated Double Channel Analysis for Petrochemical Applications."
Law, C.K., 2006. Combustion Physics. Cambridge University Press, New York.
Lawes, M.J., Richards, A., 2011. Bark thickness determines fire resistance of selected tree species from fire-prone tropical savanna in north Australia. Plant Ecol. 212, 2057–2069.
Leroy, V., Cancellieri, D., Leoni, E., 2006. Thermal degradation of ligno-cellulosic fuels: DSC and TGA studies. Thermochim. Acta 451 (1–2), 131–138.
Liang, L., Hawbaker, T.J., Zhu, Z., Li, X., Gong, P., 2016. Forest disturbance interactions and successional pathways in the Southern Rocky Mountains. For. Ecol. Manag. 375, 35–45.
López-Martín, M., González-Vila, F.J., Knicker, H., 2018. Distribution of black carbon and black nitrogen in physical soil fractions from soils seven years after an intense forest fire and their role as C sink. Sci. Total Environ. 637–638, 1187–1196.
Mastrolonardo, G., et al., 2017. Size fractionation as a tool for separating charcoal of different fuel source and recalcitrance in the wildfire ash layer. Sci. Total Environ. 595, 461–471.
Meigs, G.W., Zald, H.S., Campbell, J.L., Keeton, W.S., Kennedy, R.E., 2015. Do insect outbreaks reduce the severity of subsequent forest fires? Environ. Res. Lett. 11.
Meredith, W., et al., 2012. Assessment of hydropyrolysis as a method for the quantification of black carbon using standard reference materials. Geochim. Cosmochim. Acta 97, 131–147.
Ohlson, M., Dahlberg, B., Økland, T., Brown, K.J., Halvorsen, R., 2009. The charcoal carbon pool in boreal forest soils. Nat. Geosci. 2 (10), 692–695.
Page, W., Jenkins, M.J., 2007. Predicted fire behavior in selected mountain pine beetle-infested lodgepole pine. For. Sci. 53 (6), 662–674.
Pérez-Ramirez, Y., Santoni, P., Darabiha, N., Leroy-Cancellieri, V., Leoni, E., 2012. A global kinetic model for the combustion of the evolved gases in wildland fires. Combust. Sci. Technol. 184 (9), 1380–1394.
Pinard, J., Huffman, M., 1997. Fire resistance and bark properties of trees in a seasonally dry forest in eastern Bolivia. J. Trop. Ecol. 13 (5), 727–740.
Preston, C.M., Schmidt, M.W.I., 2006. Black (pyrogenic) carbon: a synthesis of current knowledge and uncertainties with special consideration of boreal regions. Biogeosciences (3), 397–420.
Pyne, R.D., Stephan, J., Andrews, Patricia, L., Laven, 1996. Introduction to Wildland Fire. Wiley.
W. S. Rasband, "ImageJ," (Bethesda, Maryland, USA).
Reed, D.E., Ewers, B.E., Pendall, E., 2014. Impact of mountain pine beetle induced mortality on forest carbon and water fluxes. Environ. Res. Lett. 9.
Rumpel, C., Leifeld, C., Santin, J., 2015. Movement of biochar in the environment. Biochar for Environmental Management: Science, Technology and Implementation, 2nd ed. Routledge, Tatlor & Francis, London and New York, pp. 283–299.
Santín, C., Doerr, S.H., Preston, C.M., González-Rodríguez, G., 2015. Pyrogenic organic matter production from wildfires: a missing sink in the global carbon cycle. Glob. Chang. Biol. 21 (4), 1621–1633.
Santín, C., et al., 2016. Towards a global assessment of pyrogenic carbon from vegetation fires. Glob. Chang. Biol. 22 (1), 76–91.
Santín, C., et al., 2017. Carbon sequestration potential and physicochemical properties differ between wildfire charcoals and slow-pyrolysis biochars. Sci. Rep. 7 (1), 1–11.
Sawyer, R., Bradstock, R., Bedward, M., Morrison, R.J., 2018. Fire intensity drives post-fire temporal pattern of soil carbon accumulation in Australian fire-prone forests. Sci. Total Environ. 610–611, 1113–1124.
Schimmelpfennig, S., Glaser, B., 2011. One step forward toward characterization: some important material properties to distinguish biochars. J. Environ. Qual. 41 (September 2014).
Simard, M., Romme, W.H., Griffin, M.G., Jacob, M., Turner, 2011. Do mountain pine beetle outbreaks change the probability of active crown fire in lodgepole pine forests? Ecol. Monogr. 81 (1), 3–24.
Solheim, H., Krokene, P., 1998. Growth and virulence of mountain pine beetle associated blue-stain fungi, Ophiostoma clavigerum and Ophiostoma montium. Can. J. Bot. 76, 561–566.
L. M. Srivastava, Anatomy, Chemistry, and Physiology of Bark, vol. 1. Academic Press Inc.
Tihay, V., Gillard, P., 2011. Comparison of several kinetic approaches to evaluate the pyrolysis of three Mediterranean forest fuels. Int. J. Therm. Sci. 20 (3), 407–417.
Tihay, V., Santoni, P.-A., Simeoni, A., Garo, J.-P., Vantelon, J.-P., 2009. Skeletal and global mechanisms for the combustion of gases released by crushed forest fuels. Combust. Flame 156 (8), 1565–1575.
Verón, Santiago R., Jobbágy, Esteban G., Di Bella, Carlos M., Paruelo, José M., Jackson, R.B., 2012. Assessing the potential of wildfires as a sustainable bioenergy opportunity. GCB Bioenergy 4, 634–641.